A New Antibacterial N -Halamine Coating Based on Polydopamine

Nadia Nazi, Vincent Humblot, Catherine Debiemme

A New Antibacterial N-halamine Coating Based on Polydopamine.

Nadia NAZI[1,2], Vincent HUMBLOT*[1,3], Catherine DEBIEMME-CHOUVY*[2]

[1] Sorbonne Université, Laboratoire de Réactivité de Surface, UMR CNRS 7197, 4 place Jussieu, 75005 Paris, France

[2] Sorbonne Université, Laboratoire Interfaces et Systèmes Electrochimiques, UMR CNRS 8235, 4 place Jussieu, 75005 Paris, France

[3] FEMTO-ST Institute, UMR CNRS 6174, Université Bourgogne Franche-Comté, 15B avenue des Montboucons, 25030 Besançon Cedex, France

KEYWORDS Dopamine oxidation, Polydopamine, Chlorination, N-halamine, Antibacterial coating, Escherichia coli

ABSTRACT

To prevent the formation of biofilm on material surface, the latter must have antibacterial properties. The aim of this study is to investigate the synthesis and the antibacterial effect of a new N-halamine coating based on polydopamine (PDA). The interests of this coating are multiple, notably the green process used to prepare it and the wide variety of organic or inorganic materials that can be functionalized. First the formation of the PDA coating by oxidative polymerization of dopamine in weak alkaline aqueous solution was studied and characterized. Then, these PDA films were exposed to a NaOCl solution in order to form chloramine functions into the coating, i.e. to immobilize oxidative chlorine on and into the coating. The PDA film chlorination was notably followed in situ by quartz crystal microbalance (QCM). The influence of the NaOCl solution pH and concentration on chlorination kinetics and on PDA film degradation was evidenced. Finally, the antibacterial properties of the modified PDA coatings were highlighted by testing their anti-adhesion and bactericidal properties towards Escherichia coli bacterial strain.

INTRODUCTION

Bacterial biofilms are formed by communities that are embedded in a self-produced matrix of extracellular polymeric substances[1-3], it is a complex system in which bacteria differ radically from those of planktonic cells exhibiting new properties. An important emergent property of biofilms is the ability to survive exposure to antimicrobial compounds, including disinfectants, toxic metals and small-molecule antibiotics. In fact, bacteria in a biofilm can be 10 to 1000 times more resistant to antimicrobial agents[4]. The first step in the formation of a biofilm is the adsorption of proteins usually required for the bacterial adhesion. Then the bacterial cells will multiply and form microcolonies initially in a reversible association followed by an irreversible adhesion. The final step in the formation of a biofilm is the detachment and dispersal of bacterial cells. Biofilms can be associated with infections but also responsible for biofouling and contamination of process water, deterioration of the hygienic quality of drinking water and biocorrosion[5, 6]. This poses a real public health problem, economic or even environmental in view of the use of biocidal agents to prevent the development of biofilms.

As a result, the development of antimicrobial coatings has attracted substantial academic and industrial interests. Especially N-halamine based coatings have been extensively studied over the past decade thanks to their properties such as being one of the most powerful biocides toward a broad spectrum of microorganisms, their stability, their non-toxicity to humans and their regenerability[7-10]. An N-halamine organic polymer contains nitrogen–halogen covalent bonds, the halogen is at the oxidation state +I that confers to the coating oxidative properties. Actually, very often the antimicrobial properties of an N-halamine compound are the result of the direct transfer of chlorine (Cl(+I)) to receptors in the microorganisms[9, 11-14]. As a result, coatings containing

chloramine functions appear as very promising antibacterial rechargeable materials[15], and some of them have also been studied for their interesting antiadhesive properties[16].

To prepare an N-halamine coating, a two-step route can be used: first, the immobilization on the material surface of a polymer containing N atoms bearing an H atom followed by a treatment with an NaOCl aqueous solution to form chloramine functions by a substitution reaction:

$$>N\text{-}H + OCl^- \rightarrow >N\text{-}Cl + OH^- \quad (1)$$

Thus, to obtain an N-halamine coating, the material surface should be covered with a polymer containing primary or secondary amine functions, or primary imine or amide groups[17-20]. Herein we report a simple and practical approach in which chloramine functions were formed into a polydopamine (PDA) coating. Inspired by the adhesive nature of catechols and amines invertebrate mussel adhesive proteins, polydopamine is a simple compound to functionalizing virtually all types of material surfaces[21-23]. In fact, Nature is a source of inspiration for surface chemistry, the protein composition of mussel byssal thread near the plaque/substrate interface reveal 3,4-dihydroxy-L-phenylalanine (DOPA) and lysine-enriched proteins that is the key of the robust adhesion[24]. So, the presence of both catechol and amine groups appears to be a critical factor for efficient formation of a robust, strongly adhesive coating based on catechol chemistry applied from aqueous solution[25]. In solution, PDA film can be formed from dopamine monomer under weak alkaline conditions through a spontaneous self-assembly and oxidative cross-linking process with dioxygen as the oxidant[21, 26-28].

The advantage of polydopamine is that it can be easily deposited on virtually all types of inorganic and organic substrates, including superhydrophobic surfaces[29-31]. Moreover, these bioinspired PDA films are chemically and structurally indistinguishable from eumelanins found in the human body providing excellent biocompatibility[32].

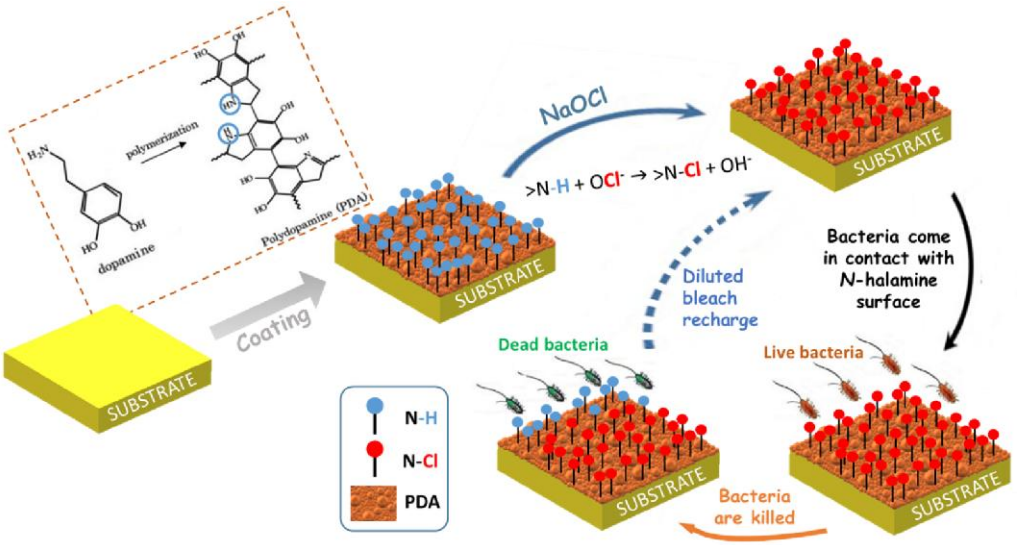

Figure 1. General strategy of formation and regeneration of an N-halamine coating based on polydopamine.

In the present work, the synthesis of PDA coating containing chloramine functions is ~~reported~~ studied in-depth for the first time. For this purpose, first, the PDA film formation on gold surfaces was performed by simple immersion of the substrate in a dopamine solution at pH 8.5. The PDA film growth was monitored in situ by means of a quartz crystal microbalance (QCM). Then, the films were characterized by Polarization-Modulation Reflection Absorption InfraRed Spectroscopy (PM-RAIRS) and X-Ray Photoelectron Spectroscopy (XPS) analyses and by Scanning Electron Microscopy (SEM) observations. The chlorination of PDA films was performed by their immersion in a NaOCl aqueous solution (reaction 1) in order to immobilize Cl(+I), oxidative species, into the polymers. The whole functionalization process is illustrated in Figure 1. Finally, antibacterial assays towards Escherichia coli were conducted to establish the antiadhesive and bactericidal properties of such N-halamine PDA-based coatings. One can note that concomitantly to this work, Chien and Chiu have studied the antibacterial and regenerability properties of chlorinated PDA film deposited on polyester fibers[33].

EXPERIMENTAL SECTION

Materials. Dopamine hydrochloride (98% purity), tris(hydroxylmethyl)aminomethane hydrochloride (Tris-HCl), phosphate buffer saline (PBS) were obtained from Sigma-Aldrich. A household bleach solution at 2.6% of active chlorine was diluted before used for the chlorination of the PDA films. Ultrapure water was obtained from a Milli-Q system (Millipore, resistivity >18 MΩ cm^{-1}) from EMD Millipore Corp. (Billerica, MA, USA). Glass substrates (11 mm × 11 mm) coated with a 5 nm thick layer of chromium and a 200 nm thick layer of gold were purchased from Arrandee (Werther, Germany). Before PDA coating, the gold-coated substrates were annealed in a butane flame to obtain a crystal reconstruction of the first atomic layers, a UV-ozone cleaning procedure for15 min was then applied prior to ultrapure water and absolute ethanol rinsing for period of 10 min each[34]. Thermanox plastic coverslips (TMX) purchased from Thermo scientific were used as reference substrates for antibacterial tests.

PDA coating. For the polydopamine coating formation, the substrates were immersed into dopamine solution, prepared by dissolving 0.5 mg/mL dopamine hydrochloride in 10 mM Tris-HCl at pH 8.5, under stirring except for QCM experiments which were performed under static conditions. Then substrates were washed with deionized water for 5 minutes under sonication and then nitrogen-dried.

PDA film chlorination. For chlorination, PDA films were soaked in 1 mM NaOCl solution at pH 10, unless otherwise stated, at room temperature. After chlorination, the substrates were washed with deionized water thoroughly and nitrogen-dried. The PDA films used for this step were either obtained after 3 h or 24 h of immersion in the dopamine solution. Before chlorination they are named PDA-3h and PDA-24h, respectively and PDA-3h-Cl and PDA-24h-Cl, respectively after chlorination.

Polarization Modulation Reflection Absorption InfraRed Spectroscopy (PM-RAIRS). PM-RAIRS measurements were carried on a Nicolet Nexus 5700 FT-IR spectrometer (Madison, WI, USA) equipped with a wide band HgCdTe detector cooled with liquid nitrogen. Infrared spectra were obtained by coaddition of 128 scans at 8 cm^{-1} resolution. A ZnSe photoelastic modulator and a ZnSe grid polarizer were placed prior to the sample to modulate the incident beam between p and s polarizations (PM90, HINDS Instruments Inc., Hillsboro, OR, USA), modulation frequency was 36 kHz. Interferograms (sum and difference) were processed via Fourier-transformation to obtain the resulting PM-RAIRS signal, which is the differential reflectivity $\Delta R/R° = (Rp-Rs)/(Rp+Rs)$, with Rs and Rp being the signals perpendicular and parallel to the incident plane, respectively.

Ellipsometry. Ellipsometry measurements were performed using a monowavelength ellipsometer SENTECH SE 400 equipped with a He–Ne laser at $\lambda = 632.8$ nm, the incident angle was 70°. All measurements are taken on nitrogen-dried samples in ambient air. The values of ns and ks used for the gold substrate were 0.2098 and 3.2852, respectively. For each sample, at least 5 measurements were performed in different zones. Therefore, the thickness values are given as the average over 5 values.

X-ray Photoelectron Spectroscopy (XPS). XPS analyses were performed using an Omicron Argus spectrometer (Taunusstein, Germany) equipped with a monochromated Alk_{α} X-ray source ($h\nu = 1486.6$ eV) working at an electron beam power of 300 W. Photoelectron emission was analyzed at a take-off angle of 45°. For angle-resolved XPS (AR-XPS), the other angles were 15° (grazing emission) and 90° (normal emission) with respect to the sample surface. The analyses were carried out under ultra-high vacuum conditions ($\leq 10^{-10}$ Torr) after introduction via a load-lock into the main chamber. Spectra were obtained by setting up a 100 eV pass energy for the

survey spectra and a pass energy of 20 eV was chosen for the high-resolution regions. Element peak intensities were corrected by Scofield factors[35]. CasaXPS software (Casa Software Ldt, UK) was used to decompose XPS spectra using a Gaussian/Lorentzian ratio 70/30.

Quartz Crystal Microbalance (QCM). QCM measurements were performed using a labmade QCM device under static conditions and a 9 MHz-gold patterned quartz substrate (S = 0.2 cm^2). The quartz were placed perpendicular to the bottom of the container. Frequency changes (Δf) of the quartz crystal resonator was monitored. The Δf was converted into the mass change (Δm) of the quartz crystal by applying the Sauerbrey equation[36]:

$$\Delta f = - \frac{}{} \Delta m \qquad \text{(Eq. 1)}$$

where A is the active surface of the gravimetric sensor, p_q is the quartz density, μ_q is the quartz shear modulus, and f_0 is the fundamental resonance frequency of the quartz.[37] We note:

$$\Delta f = -C\,\Delta m \qquad \text{(Eq. 2)}$$

with C, the experimental sensitivity constant, 16.31 10^7 Hz g^{-1} cm^2 for 9 MHz[37].

Chloramine function quantification. The presence of chloramine functions was confirmed by measuring the bleaching of a 5-thio-2-nitrobenzoic acid (TNB) solution, at 412 nm[38]. Fresh TNB solution was produced before each experiment via addition of 2 equivalents of cysteine (Cys) to 1 equivalent of 5,5'-dithiobis (2-nitrobenzoic acid) (DTNB) following the reaction:

$$\text{DTNB} + 2\ \text{Cys} \rightarrow 2\ \text{TNB} + \text{cystine} \qquad (2)$$

For this aim, in equal volumes, 2 10^{-3} M of cysteine and 10^{-3} M of DTNB were mixed in 50 mM phosphate buffer solution (PBS) at pH 7.4 giving a highly colored yellow/orange solution [39]. Then this stock solution was diluted 10-fold with 50 mM PBS, pH 7.4. The different subtracts were immersed in this solution for twenty hours. The yellow-colored TNB reacts with haloamine functions to regenerate colorless DTNB, according to Scheme S1.

The UV/visible absorbance measurements were carried out using spectrometer with 1 cm path length cuvettes. According to Beer-Lambert's law, the density of chloramine functions (d_{Cl}), in at/cm^3, was calculated thanks to the following equation:

$$d = \frac{A_{PDA} - A_{PDA\text{-}Cl}}{\varepsilon \cdot l} \cdot \frac{V_{TNB}}{V_{coating}} \cdot N_A \qquad \text{(Eq. 3)}$$

where A_{PDA} and $A_{PDA\text{-}Cl}$ are the absorbance of the TNB solution containing the substrate with the PDA coating and with the chlorinated PDA coating, respectively, ε = 14100 $M^{-1}.cm^{-1}$, l = 1 cm, $V_{coating}$ is the volume of the PDA film in cm^3, V_{TNB} is the volume of the TNB solution in L and N_A is Avogadro constant.

SEM observations. The surfaces or cross-sections of the PDA films were examined under an Ultra55 Zeiss field-emission-gun scanning electron microscope (FEG-SEM), operating at 10 kV. For the cross section observations, the samples were tilted (60°).

Bacterial strain and culture conditions. Bacteria Escherichia coli ATCC 25922 were used to investigate the antibacterial properties of the chlorinated PDA films. Bacterial suspensions were prepared from frozen cultures incubated overnight (37°C under agitation at 250 rpm) in Luria-Bertani (LB) broth (BD Difco, Franklin Lakes, NJ, USA).

Evaluation of bacterial adhesion. Substrates were put into sterile Petri dishes in the presence of 20 mL of bacteria suspension at 10^6 CFU/mL in PBS, under stirring at room temperature for 17 h. After incubation, for evaluation of bacterial adhesion, an optical microscopy analyze was performed. For this, the samples were rinsed with PBS, stained for 5 minutes with 1 mL of crystal violet at 1% (w/w), rinsed under water flow until color loss and dried. For each sample, the surface density of bacteria was determined by averaging 20 microscope fields under a 50x magnification. Results were expressed as a percentage of the attached bacterial cells onto the different PDA surfaces, as compared to TMX substrates.

Bacteria Growth Capacity (cultivability of adhered bacteria). Bacterial growth capacity after contact with functionalized surfaces was determined performing killing tests. Before bacterial inoculation, the surfaces were sterilized by washing them five times with ethanol solution at 70 %. The killing test was performed in sandwich configuration. For this, 20 µL of the bacterial suspension in PBS media were deposited on a first plate then a second plate is placed onto the first one, on the coating side so that the bacterial suspension is sandwiched between the two substrates. After 3 hours of contact at room temperature, surfaces were transferred into a tube containing 2 mL of sterile PBS solution and sonicated (Bandelin Sonorex RK 31, Berlin, Germany; f = 35 kHz, P = 90 W) for 2 min to recover the adhered bacteria without damaging them. After the sonication, SEM-FEG observations of the plates were performed to verify that most of the adhered bacteria were detached during the sonication process. The recovered bacteria suspensions were diluted 10, 10^2, 10^3 and 10^4 times before deposition of 20 µL of each dilution in triplicate on LB-agar plates. The plates were incubated at 37 °C overnight before enumeration. Results were expressed in number of attached and cultivable bacterial cells onto the different surfaces per mL (CFU/mL). Each test was done in triplicate, the number of CFU/mL is the average of the results obtained for each sample.

RESULTS AND DISCUSSION

PDA coating elaboration

In solution, dopamine within the right conditions of pH is known to oxidize and self-polymerized, this is evidenced by a change of solution color, from colorless to dark brown[40]. In this study, the bare gold surfaces were dipped into a dopamine solution in which Tris-HCl is added after a few minutes. The surface dopamine-polymerization process was followed in situ using a quartz crystal microbalance, and ex situ by means of PM-RAIRS as a function of the immersion time.

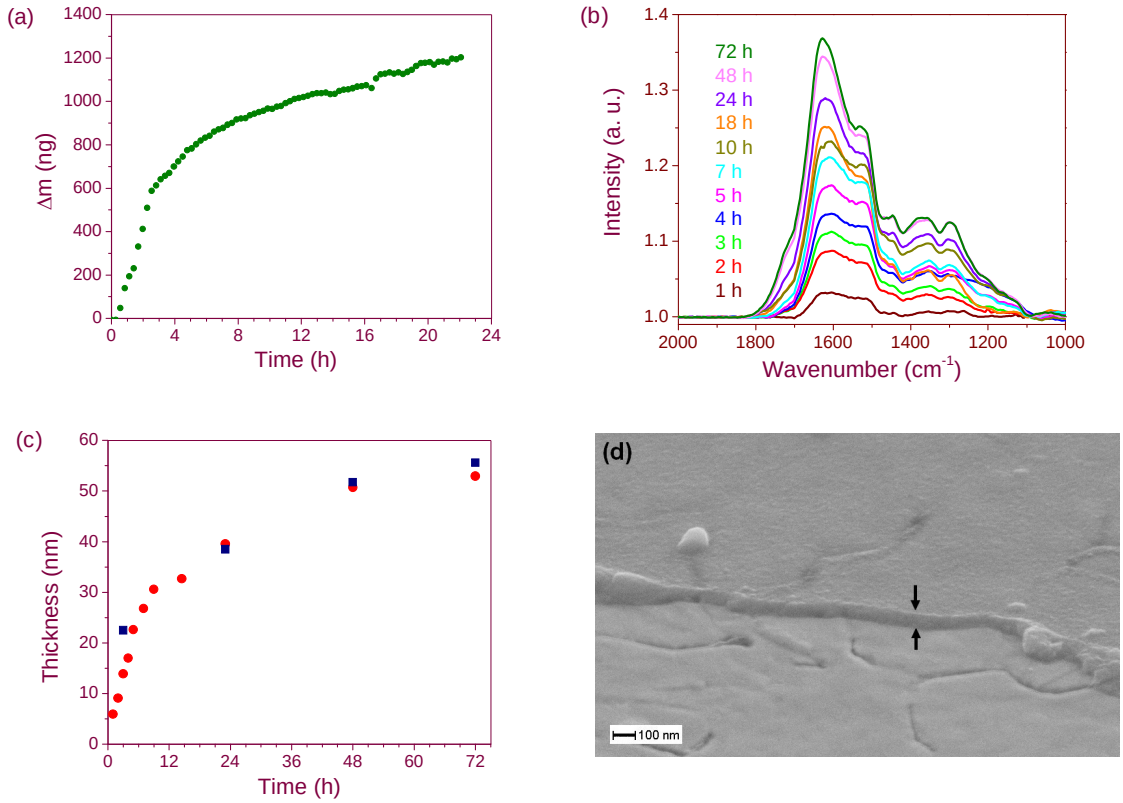

Figure 2. PDA coating formation in a 0.5 mg/mL dopamine solution. (a) QCM investigation of PDA coating formation in the dopamine solution, dopamine was added after 0.5 h in the Tris-HCl solution. (b) PM-RAIRS spectra of gold surfaces functionalized with a PDA film by immersion in the dopamine solution for various times. (c) PDA film thickness evaluated by ellipsometry (red circles) and SEM analysis (blue squares). (d) SEM micrograph of a PDA coating on gold substrate after 72 h of immersion in the dopamine solution.

Figure 2(a) shows the QCM response whereas Figure 2(b) presents the IR spectra obtained for gold surfaces immersed for different times ranging from 1 h up to 72 h. A broad IR massif is observed in 1600 cm^{-1} region which intensity increases as a function of immersion time. A second group of features is visible at lower wavenumbers. No other IR feature are detected whatever the exposure time. All these features indicate the presence of dopamine intermediate and polydopamine film, with the main characteristic peaks observed at 1620 and 1515 cm^{-1}, assigned

to ν_{ring}(C=C) and ν(N-H) vibrations[41], respectively. Secondary IR peaks are also observed at lower wavenumbers, namely 1450, 1350 and 1290 cm^{-1}, assigned to the stretching vibration ν_{ring}(CNC), but also to vibrations related to remaining catechol groups of free dopamine, ν(C-O) and ν(C=N)[42-44]. These IR features are consistent with those obtained for PDA in solution (data not shown) and thus, the PM-RAIRS analyses clearly indicate the formation of PDA coating on gold surfaces.

PDA film growth can be quantitatively investigated on one hand using PM-RAIRS data, by integrating the peak areas as a function of immersion time, as presented in Fig. S1, on the other hand using QCM analysis as presented in Fig. 2(a). Meanwhile, data collected on the same samples by ellipsometry enabled to obtain average thickness for the PDA films using an appropriate model for gold surfaces, Fig. 2(c). These values were confirmed by SEM observations of the cross-section of the samples (Fig. 2(d)).

PM-RAIRS analysis (Fig. S1), QCM (Fig. 2a) and thickness measurements (Fig. 2c) show that the growth of the PDA film as function of the substrate immersion time follows a logarithmic function, with a growth rate about 5 nm/h during the first hours (Fig. 2c). The combination of the PDA mass obtained by QCM (1.2 μg for 24 h of immersion) and of its thickness obtained by ellipsometry and SEM observation (40 nm for 24 h of immersion) allowed us to estimate the density of the PDA film i.e. 1.49 g cm^{-3}. This finding is in good agreement with value reported in the literature[45]. Moreover ellipsometry data show that the PDA thickness on gold substrates gradually reached a constant value of around 50 nm after 48 hours of immersion, which is within the range of PDA film thicknesses reported in Ref. 21. This stationary phase is mainly due to the depletion of dopamine monomer in the supernatant solution, being able to cross link onto the PDA film, into the profit of the non-reactive quinone molecules[46]. For the characterizations, the chlorination

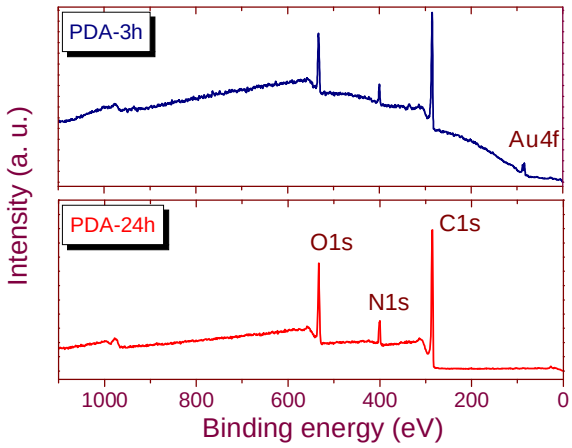

Figure 3. XPS survey spectra of gold surfaces coated with PDA films after 3 h (blue line, top spectrum) and 24 h (red line, bottom spectrum) of immersion in a 0.5 mg/mL dopamine solution.

experiments and the biological tests of the PDA films, two synthesis times have been chosen: 3 hours and 24 hours.

XPS analysis were thus performed on these 2 sets of PDA coated Au surface, the survey spectra are presented in Fig. 3. For PDA-24h sample, the photopeaks C1s (285 eV), O1s (530 eV) and N1s (400 eV) are observed whereas Au 4f contribution (84 eV) is not detected on the contrary to the sample coating with a PDA film formed for 3 hours (Fig. 3). For both samples, the chemical composition in carbon and nitrogen is close to the theoretical composition of polydopamine (N/C= 0.125) taking into account the carbon contamination which slightly reduces the N/C ratio (Table 1), thus confirming the results obtained by PM-RAIRS (growth of a PDA film). Concerning the PDA film thickness evaluated from XPS data, they are in good agreement with those obtained by ellipsometry. Indeed, for PDA-24h coating the XPS Au4f signal is not detected suggesting an equivalent thickness higher than $3\lambda = 12$ nm representing 95% of signal, λ being the inelastic mean free path of electrons in the organic PDA film, for electrons having a kinetic energy around 1400

eV (from Au4f atomic level) λ is estimated to be equal to 3.62 nm[47]. For PDA-3h coating, the Au4f signal is weak but still visible (Fig. 3), indicating an equivalent thickness close to 12 nm, again in good agreement with the value of 15 nm obtained by ellipsometry.

Table 1. Chemical composition in at% of PDA-coated gold surfaces obtained from XPS data presented in Figs. S2 and 5 and ratio between N and C and Cl_{200} and N. Cl_{198} corresponds to Cl^- and Cl_{200} to chloramine.

	C	N	O	Au	N/C	Cl_{198}	Cl_{200}	Cl_{200}/N
PDA-3h	76.3	7.2	16.2	0.3	0.094	-	-	-
PDA-24h	75.3	7.2	17.1	-	0.095	-	-	-
PDA-3h-Cl	69.4	5.7	19.4	1.15	0.082	0.6	3.9	0.68
PDA-24h-Cl	69.85	6.45	18.9	-	0.092	0.78	4.0	0.62

PDA film chlorination

The chlorination of the PDA films was performed by immersion of the sample in NaOCl solution. It is known that long contact time with acidic solution or alkaline solutions could denature the PDA films[48-50]. Since the chlorination will take place in NaOCl solutions at pH around 10, it is possible that after a given time, the PDA film will start to degrade. In situ monitoring by QCM was first conducted at different NaOCl concentrations: 0.2 mM, 1 mM and 10 mM to evaluate the influence of the concentration in sodium hypochlorite and then estimate the time until which it is safe to put in contact the PDA films with the NaOCl solution. Tests were also done at pH 7. For this pH value, for a 1 mM NaOCl concentration, similar results (see Fig. S3c) were obtained than at pH 10 but with slower kinetics in good agreement with lower concentration of hypochlorite ions at pH 7 than at pH 10 ($pK_a(HOCl/OCl^-) = 7.5$). Note that at pH 5 no chlorination occurs, confirming that the species responsible for chlorination are OCl^- ions. These findings are summarized in Table 2.

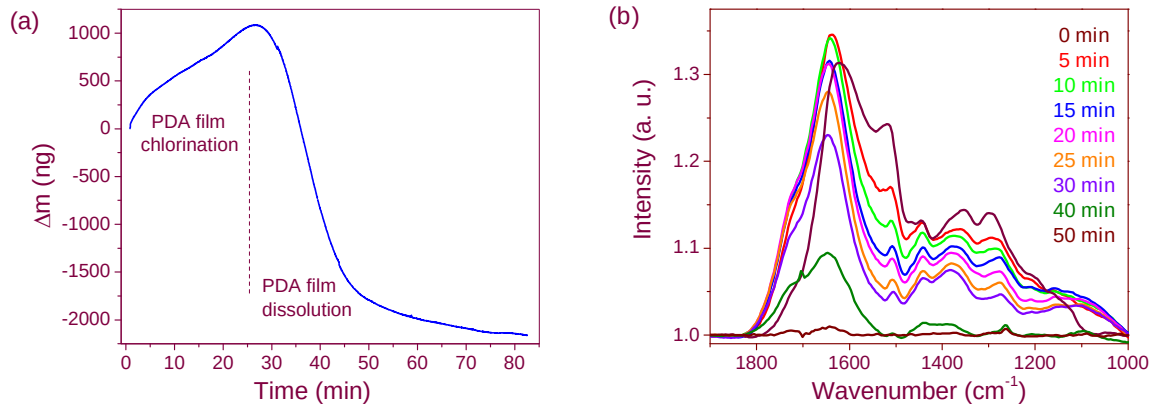

Figure 4. PDA film chlorination. (a) QCM investigation of the PDA-24h film chlorination in 1 mM NaOCl solution, pH = 10. Quartz surface: 0.2 cm^2. (b) PM-RAIRS spectrum of gold surface coated with a PDA-24h film as a function of exposure time to a 1 mM NaOCl solution, pH = 10.

The chlorination of a PDA-24h film in 1 mM NaOCl solution was studied by QCM, the response mass variation vs. contact time is shown in Fig. 4a. The data obtained for other NaOCl concentrations are presented in Fig. S3. Obviously, the mass increase has been ascribed to chlorine fixation on and into the PDA film (reaction 1). For solution at pH 10, whatever the sodium hypochlorite concentration, the shape of the mass variation (Δm) vs. time is the same. Namely, first the film mass increases rapidly then progressively reaches an optimal mass increase corresponding to an optimal chlorination time in NaOCl solution. Actually, there are two kinetic regimes. We can assume than the first one, at the beginning, corresponds to the chlorination of the PDA film surface with a kinetic limitation by the OCl^- diffusion in the bulk of the solution whereas the second one, slower, corresponds to the chlorination of the film with a kinetic limitation by the OCl^- diffusion inside the polymer. One can notice that for pH 7, the response is different, this can be due to an increase at the film/solution interface of the pH due to OH^- release (reaction 1) and therefore to an increase of the interfacial concentration of OCl^- ions.

Table 2. QCM results. Times in minutes at which (i) the maximal mass increase is reached and (ii) the PDA film is entirely degraded (removed from the substrate surface), for PDA-24h films in contact with ~~a~~ NaOCl solutions of various Cl(+) (HOCl and/or OCl^-) concentrations, pH and initial OCl^- concentration (data from Figs. 4a and S3).

[Cl(+)] (mM)	0.2	1	1	1	10
pH	10	10	7	5	10
$[OCl^-]$ (mM)	0.2	1	0.24	0	10
$t_{\Delta m\ max}$ (min)	156	25	35	no mass variation	7
$t_{Degradation}$ (min)	360	60	65	stable	11

After that, the mass decreases down to a value lower than the initial one. This finding can be explained by the degradation of the PDA coating upon long exposure to the NaOCl solution. In addition, the substitution mechanism of H by Cl(+I) (reaction 1) leads to the release of hydroxyl ions thus to an increase of the interfacial pH, that could result in progressive degradation of the PDA film. For pH 10, the optimal time of chlorination is function of the NaOCl concentration, this time decreases with the increase in the concentration passing from 156 min for a concentration of 0.2 mM to 25 min for 1 mM and finally 7 min for 10 mM (Table 2). From Table 2 one can notice that the PDA film degradation/dissolution kinetics is also function of the OCl^- ion concentration, the higher the anion concentration the faster the degradation of the PDA film is.

For the present study, the NaOCl concentration of 1 mM was chosen. In this condition, as shown in Fig. 4a, the maximal Δm is 1080 ng. Thus the chlorine amount fixed into the PDA film is estimated to be $1.89\ 10^{16}$ atoms and taking into account a film thickness of 40 nm (according to Fig. 2c), a Cl atom density (d_{Cl}) equals to $2.3\ 10^{22}$ at cm^{-3} is obtained (equation 4). If we compare this result with the theoretical N density in PDA that is $5.3\ 10^{21}$ at cm^{-3}, an overestimation of the

chlorine density is obtained with QCM. Moreover, the N/Cl ratio obtained by XPS analysis (Table 3) is inferior to 1 indicating that the number of Cl atoms is lower than the one of N atoms in the chlorinated PDA film. Since Na is detected by XPS at 1071 eV (Fig. 5) even after rinsing the samples it is obvious that the mass variation is not only due to H substitution by Cl (reaction 1). Therefore in the present case a quantification of N-Cl groups by QCM is not possible.

$$= \frac{\qquad\qquad}{(\qquad)} \qquad \text{(Eq. 4)}$$

where M is the molecular mass, S is the quartz surface (0.2 cm^2) and e_{PDA} is the thickness of the PDA film.

To complete the study by QCM, an ex situ study was carried out by PM-RAIRS for PDA-3h coating (Fig. S4) and PDA-24h coating (Fig. 4b). First, after chlorination there is a change of the PDA IR spectrum. The spectrum reveals a sharp decrease in the peak at 1515 cm^{-1} attributed to the N-H group and which therefore suggests the creation of chloramine functions. A shift of the characteristic peak of the aromatic passing from 1620 cm^{-1} to 1645 cm^{-1} is also noticed. This shift can be a consequence of the grafting of chlorine atoms on nitrogen atoms located near the aromatic cycle modifying the chemical environment of the latter. Finally, the appearance of a shoulder around the 1720 cm^{-1} that increases over chlorination time is observed, it could be due to the appearance of carboxylic functions due to the oxidation of the PDA coating.

Regarding the kinetic monitoring of chlorination, the results of the QCM study are confirmed. Namely, for a 1 mM NaOCl solution at pH 10 an optimal chlorination time around 25 minutes is determined, indeed after this time a strong decrease in the intensity of the peaks characteristic of the PDA is observed until a complete disappearance after 50 min revealing the complete degradation of the coating in agreement with the QCM results. As far as the PDA-3h coating is concerned, the optimal chlorination time was fixed at 15 min (see Fig. S4).

The chemical composition of the chlorinated PDA-3h (15 nm thick) and PDA-24h (40 nm thick) film surface was then determined by XPS. In the survey spectra, chlorine contributions are detected at binding energy around 200 eV (Cl2p) and 280 eV (Cl2s) (Fig. 5). High-resolution Cl2p spectra for PDA-3h-Cl and PDA-24h-Cl coatings are depicted in Fig. 5c and 5d, respectively, exhibiting two types of contribution. The most intense is detected at binding energy (BE) of 200.5 eV and 202.1 eV ($Cl2p_{3/2}$ and $Cl2p_{1/2}$, respectively) while the second doublet appears at lower BE, 197.6 eV and 199.2 eV. The detection of Cl2p at binding energy around 200.5 eV, named Cl_{200}, could be ascribed to N-Cl. To confirm it, a methionine test has been performed on a chlorinated PDA-24h coating. The presence of chloramines can be evidenced by methionine ($R\text{-}S\text{-}CH_3$) that reacts with chloramines according to[51, 52]:

$$R\text{-}S\text{-}CH_3 + >N\text{-}Cl + H_2O \rightarrow R\text{-}SO\text{-}CH_3 + >N\text{-}H + Cl^- + H^+ \qquad (3)$$

After contact with methionine, the $Cl2p_{3/2}$ contribution at 200.5 eV has largely decreased (data not shown) confirming that this contribution is related to chloramine bonds.

Finally, the Cl_{200} /N1s ratio for chlorinated PDA-3h and PDA-24h coatings (Table 1) reveals a similar amount of immobilized chlorine for both samples.

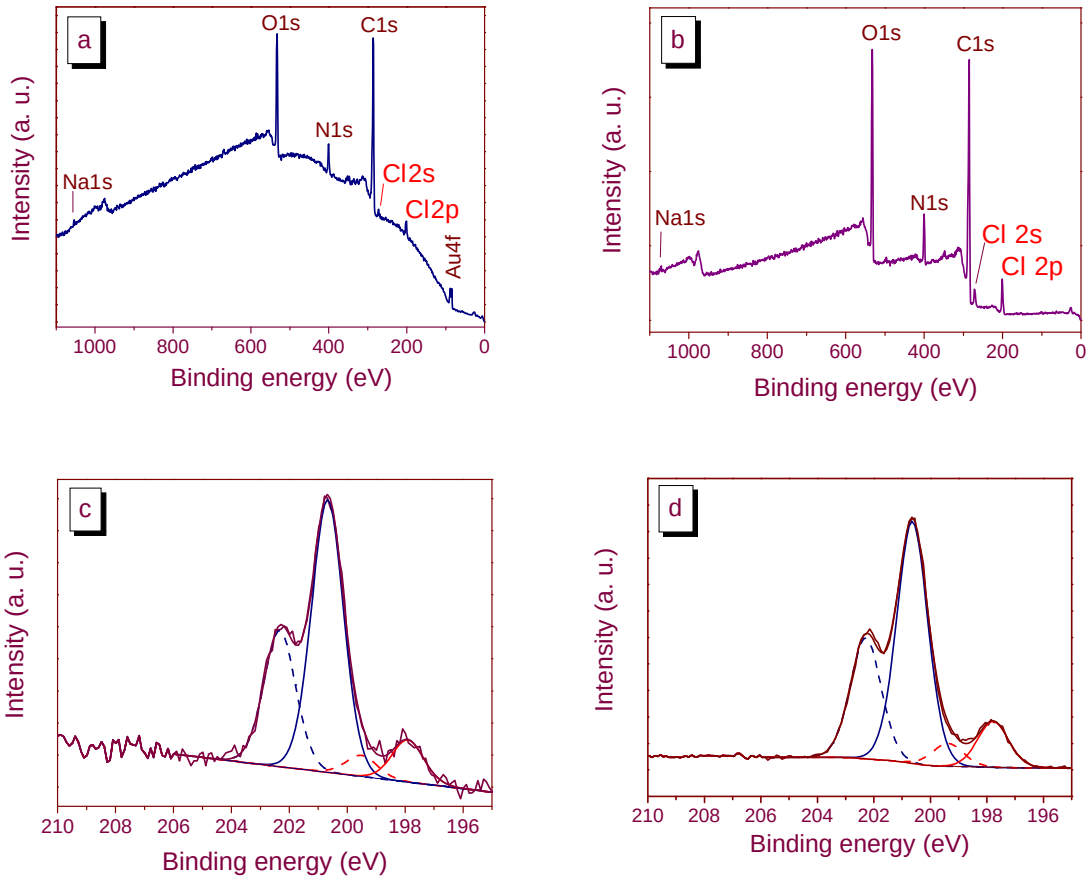

Figure 5. XPS characterizations of gold surface coated with a PDA-24h film after immersion in 1 mM NaOCl solution: (a,b) survey spectra, (c,d,) Cl2p high-resolution region. Full line: $2p_{3/2}$ contribution, dashed line: $2p_{1/2}$ contribution.

As a result of the XPS analysis, the grafting of chlorine within the PDA film is confirmed. XPS allows to analyze a film thickness about 12 nm. However by varying the angle of the electron collect i.e. performing angle-resolved XPS (AR-XPS), it is possible to decrease this thickness in order to evaluate the homogeneity of the film in depth. This analysis was done for the chlorinated PDA films. The chemical composition of the films was determined at 3 different collecting angles

(90°, 45° and 15° with respect to the sample surface), a normal emission with a bulk sensitive and at grazing emissions with a surface sensitive. Table 3 shows that whatever the electron take-off angle is, the Cl_{200}/N ratio for chlorinated PDA-3h and PDA-24h coatings are similar confirming that the PDA film chlorination occurs not only on the surface but also inside the film.

Table 3. At% ratio between Cl_{200} and N obtained by XPS at various detection angles (AR-XPS), angles are defined with respect to the sample surface for chlorinated PDA-coated gold surfaces.

	PDA-3h-Cl			PDA-24h-Cl		
Angle	15°	45°	90°	15°	45°	90°
Cl_{200}/N	0.69	0.67	0.59	0.61	0.62	0.69

The effect of the chlorination on the PDA surface morphology was studied by SEM (Fig 6). There is an evolution of the surface after chlorination with a large decrease of the PDA nanoparticles strongly linked to the surface coating since they are not removed during the sonication step. Therefore, it seems that there is a less rough surface after chlorination due to the oxidative character of OCl^- ions.

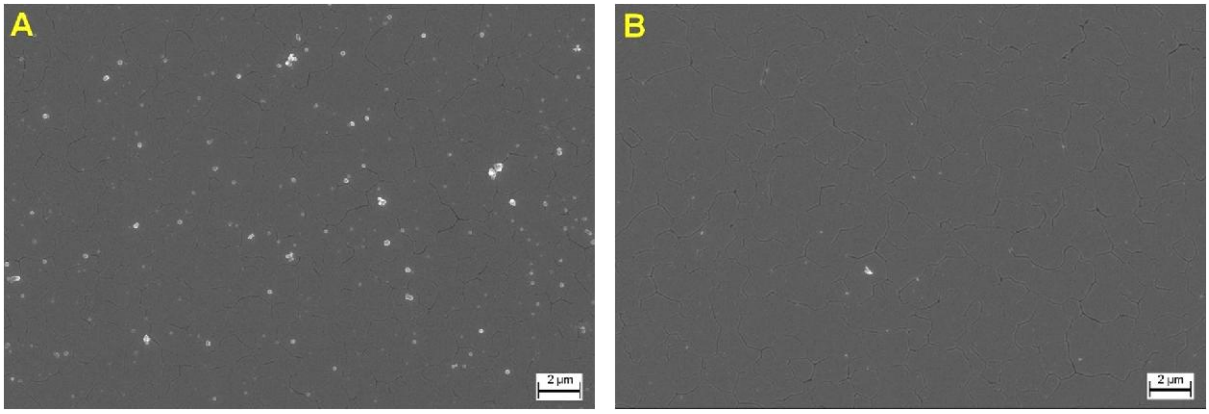

Figure 6. SEM micrographs of the PDA-24h films formed on gold subtract (A) before and (B) after immersion for 20 minutes in a 1 mM NaOCl solution pH 10.

Finally, the presence of chloramines in PDA-3h-Cl and PDA-24h-Cl coatings was evidenced by the oxidation of TNB to the corresponding dimer (DTNB) (Scheme S1). This reaction is accompanied by a loss of absorbance at 412 nm (Table 4)[38], TNB solutions are shown in Fig. S5. The amount of N-Cl bonds present into the PDA-24h-Cl film was estimated taking into account a PDA film thickness of 40 nm (according to Fig. 2c), the atom density d_{Cl} is equal to 2.5 10^{21} at cm^{-3} (Eq. 3). For the PDA-3h-Cl film, d_{Cl} is equal to 3.15 10^{21} at cm^{-3}, taking into account a film thickness of 15 nm (according to Fig. 2c). The comparison of these densities with the N density in PDA, 5.3 10^{21} at cm^{-3} taking a PDA density of 1.49 g cm^{-3}, it is thus noted that between 50 and 60% of N atoms are chlorinated, this finding confirms the XPS results (Tables 1 and 2).

Finally, after exposure in air or immersion in PBS solution (pH 7.4) for 7 days, XPS and IR analyses have revealed no change in the chemistry of the PDA-24h-Cl films. Notably the atomic ratio Cl_{200}/N is not modified, indicating that in these conditions the chlorinated PDA films are stable.

Table 4: TNB solution absorption at 412 nm after 24 h of immersion of various samples, number of chlorine atoms and density (Eq. 3) of chloramine in PDA-3h-Cl and PDA-24h-Cl coatings estimated by TNB dosage. Cl/N atomic ratio taking into account an N density of 5.3 10^{21} at.cm^{-3}.

	A at 412 nm	Cl (at.)	d_{Cl} (at.cm^{-3})	Cl/N
PDA-3h	1.38	---	---	
PDA-3h-Cl	0.9	2 10^{16}	3.15 10^{21}	0.59
PDA-24h	1.30	---	---	
PDA-24h-Cl	0.35	4.05 10^{16}	2.5 10^{21}	0.47

Antibacterial properties of chlorinated PDA films

In order to evaluate the antibacterial/antiadhesive properties of the chlorinated PDA surfaces, a suspension of Escherichia coli cells was put in contact with these surfaces and compared to negative controls, composed of first, a biocompatible neutral surface (Thermanox or TMX) and, second, the non-chlorinated PDA film.

Concerning the antiadhesive properties of chlorinated PDA films, the main results are summarized in Fig. S6 and the average data are reported in Table 5. Adhesion results from E. coli towards different surfaces reveal an antiadhesive effect of the chlorinated PDA-3h and PDA-24h coatings compared to TMX with a bacterial adhesion of 55% and 53%, respectively and compared to unchlorinated PDA corresponding, an adhesion of 55% and 67%, respectively. These results clearly show that after treatment of the PDA coatings in the presence of NaOCl, the bacterial densities on the film surface are lower. In conclusion, the PDA film chlorination provides an antiadhesive effect, up to a decrease of 45% for the best scenario.

Table 5. Mean number of Escherichia coli counted with an optical microscopy image (over 20 fields) (x50), standard deviation (σ) and calculated bacterial density, on various samples after incubation at room temperature for 17 h in the presence of 10^6 CFU/mL

Sample	TMX	PDA-3h	PDA-3h-Cl	PDA-24h	PDA-24h-Cl
Bacterial density /cm^2	970	970	540	770	520
σ	78	76	59	75	51
% adhesion (Ref: TMX)	--	100%	55%	79%	53%
% adhesion (Ref: PDA-3h or PDA-24h)	--	--	55%	--	67%

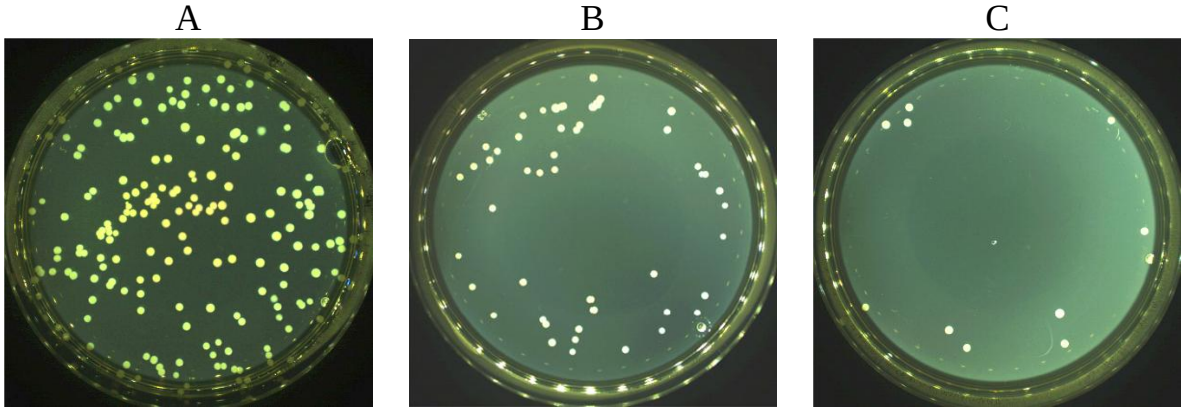

Figure 7. Optical photographs of agar plates presenting the killing test results of (A) E. coli inoculum, (B) PDA-24h and (C) PDA-24h-Cl coatings, after 3 h in contact with 20 µL of an Escherichia coli suspension at a concentration of 2.5 10^5 CFU/mL.

In addition of this antiadhesive effect of the chlorinated PDA coating, the viability of bacteria that nevertheless adhered to the films was evaluated through a killing test. A given amount of bacteria in physiological media was deposited at room temperature onto different surfaces. Under these conditions, it is important to keep in mind that bacteria cannot grow and therefore the number of bacteria counted afterwards on agar plates allows the evaluation of the viability upon contact

with the surfaces. Again, a negative control was used to asses this bacterial viability, the inoculum or the non-chlorinated PDA films. The results are shown in Fig. 7 and the average data are reported in Table S1. One can notice that both unchlorinated PDA samples, 3h and 24h, lead to a reduction of viable bacteria of 98% in comparison to the inoculum. Thus the PDA coating exhibits an antibacterial activity, this property has already been reported by Lei et al.[53] and Iqbal et al.[54]. In addition to this antibacterial effect due to the unchlorinated coating, the chlorination gives an increase of 18% of the antimicrobial activity for PDA-3h film and up to 34% for PDA-24h coating. The combination of the two antimicrobial effects leads to a bacterial viability reduction of more than 99.0% for the chlorinated PDA-3h coating and 99.5% for the chlorinated PDA-24h film in comparison with the inoculum.

CONCLUSIONS

In summary, we have demonstrated the possibility to elaborate a new antibacterial coating formed by a thin chlorinated polydopamine film. This film is obtained by dopamine monomer polymerization in weak alkaline aqueous solution followed by a treatment in a NaOCl solution. This treatment leads to the formation of chloramine functions on and inside the polymer. Chemical determinations enable to estimate the quantity of oxidative chlorine immobilized in the PDA film to be about $3\ 10^{21}$ at cm^{-3}, with a chlorination degree of N atoms between 50 et 60%, suggesting that in the PDA coating 40 to 50% of N atoms do not bear an H atom which could be exchanged with oxidative chlorine. Finally, microbiological tests towards Escherichia coli bacteria show that chlorinated PDA coatings are able to reduce E. coli adhesion up to 45 % compared to uncoated surfaces, while in the same time bacterial viability is reduced by 99% on chlorinated PDA coating.

ASSOCIATED CONTENT

Supporting Information. Scheme of the reaction between TNB and haloamine. PM-RAIRS results (2 figures). XPS high-resolution spectra of a PDA film. Chlorination followed by QCM ([NaOCl] = 0.2 mM, 10 mM at pH 10 and 1 mM at pH 7). TNB dosage. Optical images of PDA after contact with E. coli, result of the killing test (table).

AUTHOR INFORMATION

Corresponding Authors

Catherine Debiemme-Chouvy, email catherine.debiemme-chouvy@sorbonne-universite.fr

ORCID ID: 0000-0001-7171-6039

Vincent Humblot, email vincent.humblot@femto-st.fr

ORCID ID: 0000-0002-6266-3956

Author Contributions

The manuscript was written through contributions of all authors. All authors have given approval to the final version of the manuscript.

Funding Sources

This work was supported by French state funds managed by the ANR within the Investissements d'Avenir program under reference ANR-11-IDEX-0004-02, and more specifically within the framework of the Cluster of Excellence MATISSE, which provided experimental support funding for N. Nazi.

ACKNOWLEDGMENT

The authors acknowledge IPCM (Institut Parisien de Chimie Moléculaire, UMR8232), M. Laurens, for the providing access and formation to their ellipsometry apparatus and IMPC (Institut des Matériaux de Paris Centre, FR2482) and C'Nano project of Region Ile-de-France, for Omicron XPS apparatus funding.

REFERENCES

1. Costerton, J. W.; Stewart, P. S.; Greenberg, E. P., Bacterial Biofilms: A Common Cause of Persistent Infections. 1999, 284, 1318-1322.
2. Hall-Stoodley, L.; Stoodley, P., Evolving concepts in biofilm infections. 2009, 11, 1034-1043.
3. Hall-Stoodley, L.; Costerton, J. W.; Stoodley, P., Bacterial biofilms: from the Natural environment to infectious diseases. Nature Reviews Microbiology 2004, 2, 95-108.
4. Anderson, G. G.; O'Toole, G. A., Innate and Induced Resistance Mechanisms of Bacterial Biofilms. In Bacterial Biofilms, Romeo, T., Ed. Springer Berlin Heidelberg: Berlin, Heidelberg, 2008, pp 85-105.
5. Kaplan, J. B., Biofilm dispersal: mechanisms, clinical implications, and potential therapeutic uses. Journal of dental research 2010, 89, 205-218.
6. de Vos, W. M., Microbial biofilms and the human intestinal microbiome. NPJ biofilms and microbiomes 2015, 1, 15005-15005.
7. Kenawy, E. R.; Worley, S. D.; Broughton, R., The chemistry and applications of antimicrobial polymers: A state-of-the-art review. Biomacromolecules 2007, 8, 1359-1384.
8. Hui, F.; Debiemme-Chouvy, C., Antimicrobial N-halamine polymers and coatings: a review of their synthesis, characterization, and applications. Biomacromolecules 2013, 14, 585-601.
9. Dong, A.; Wang, Y. J.; Gao, Y.; Gao, T.; Gao, G., Chemical Insights into Antibacterial N-Halamines. Chem Rev 2017, 117, 4806-4862.
10. Debiemme-Chouvy, C.; Cachet, H., Electrochemical (pre)treatments to prevent biofouling. Current Opinion in Electrochemistry 2018, 11, 48-54.
11. Demir, B.; Broughton, R. M.; Qiao, M.; Huang, T. S.; Worley, S. D., N-Halamine Biocidal Materials with Superior Antimicrobial Efficacies for Wound Dressings. Molecules 2017, 22, 1582.

12. Barnela, S. B.; Worley, S. D.; Williams, D. E., Syntheses and antibacterial activity of new N-halamine compounds. Journal of Pharmaceutical Sciences 1987, 76, 245-247.
13. Worley, S. D.; Sun, G., Biocidal Polymers. rends polymer Science 1996, 4, 364-370.
14. Bai, R.; Zhang, Q.; Li, L.; Li, P.; Wang, Y.-J.; Simalou, O.; Zhang, Y.; Gao, G.; Dong, A., N-Halamine-Containing Electrospun Fibers Kill Bacteria via a Contact/Release Co-Determined Antibacterial Pathway. ACS Applied Materials & Interfaces 2016, 8, 31530-31540.
15. Gottardi, W.; Debabov, D.; Nagl, M., N-chloramines, a promising class of well-tolerated topical anti-infectives. Antimicrobial agents and chemotherapy 2013, 57, 1107-1114.
16. Ye, Q.; Zhou, F.; Liu, W., Bioinspired catecholic chemistry for surface modification. Chem Soc Rev 2011, 40, 4244-58.
17. Cao, Z. B.; Sun, Y. Y., Polymeric N-Halamine Latex Emulsions for Use in Antimicrobial Paints. Acs Applied Materials & Interfaces 2009, 1, 494-504.
18. Kocer, H. B.; Cerkez, I.; Worley, S. D.; Broughton, R. M.; Huang, T. S., N-Halamine Copolymers for Use in Antimicrobial Paints. Acs Applied Materials & Interfaces 2011, 3, 3189-3194.
19. Postma, T. M.; Albericio, F., Immobilized N-Chlorosuccininnide as a Friendly Peptide Disulfide-Forming Reagent. Acs Combinatorial Science 2014, 16, 160-163.
20. Wang, F.; Liu, M.; Ding, R.; Liang, M.; Huang, L.; Yu, J.; Si, Y., Rechargeable Antibacterial Polysulfonamide-Based N-Halamine Nanofibrous Membranes for Bioprotective Applications. ACS Applied Bio Materials 2019, 2, 3668–3677.
21. Lee, H.; Dellatore, S. M.; Miller, W. M.; Messersmith, P. B., Mussel-inspired surface chemistry for multifunctional coatings. Science 2007, 318, 426-430.
22. Liu, Y.; Ai, K.; Lu, L., Polydopamine and its derivative materials: synthesis and promising applications in energy, environmental, and biomedical fields. Chem Rev 2014, 114, 5057-115.
23. Ball, V., Physicochemical perspective on "polydopamine" and "poly(catecholamine)" films for their applications in biomaterial coatings. Biointerphases 2014, 9, 030801.
24. Waite, J. H.; Qin, X., Polyphosphoprotein from the Adhesive Pads of Mytilus edulis. Biochemistry 2001, 40, 2887-2893.
25. Lin, Q.; Gourdon, D.; Sun, C.; Holten-Andersen, N.; Anderson, T. H.; Waite, J. H.; Israelachvili, J. N., Adhesion mechanisms of the mussel foot proteins mfp-1 and mfp-3. 2007, 104, 3782-3786.

26. Lee, B. P.; Messersmith, P. B.; Israelachvili, J. N.; Waite, J. H., Mussel-Inspired Adhesives and Coatings. 2011, 41, 99-132.
27. Ball, V.; Del Frari, D.; Michel, M.; Buehler, M. J.; Toniazzo, V.; Singh, M. K.; Gracio, J.; Ruch, D., Deposition Mechanism and Properties of Thin Polydopamine Films for High Added Value Applications in Surface Science at the Nanoscale. Bionanoscience 2012, 2, 16-34.
28. Delparastan, P.; Malollari, K. G.; Lee, H.; Messersmith, P. B., Direct Evidence for the Polymeric Nature of Polydopamine. Angewandte Chemie-International Edition 2019, 58, 1077-1082.
29. Wei, Q.; Zhang, F.; Li, J.; Li, B.; Zhao, C., Oxidant-induced dopamine polymerization for multifunctional coatings. Polymer Chemistry 2010, 1, 1430.
30. Yang, H.-C.; Luo, J.; Lv, Y.; Shen, P.; Xu, Z.-K., Surface engineering of polymer membranes via mussel-inspired chemistry. Journal of Membrane Science 2015, 483, 42-59.
31. Ding, Y. H.; Floren, M.; Tan, W., Mussel-inspired polydopamine for bio-surface functionalization. Biosurface and biotribology 2016, 2, 121-136.
32. Luo, R.; Tang, L.; Zhong, S.; Yang, Z.; Wang, J.; Weng, Y.; Tu, Q.; Jiang, C.; Huang, N., In Vitro Investigation of Enhanced Hemocompatibility and Endothelial Cell Proliferation Associated with Quinone-Rich Polydopamine Coating. Acs Applied Materials & Interfaces 2013, 5, 1704-1714.
33. Chien, H.-W.; Chiu, T.-H., Stable N-halamine on polydopamine coating for high antimicrobial efficiency. European Polymer Journal 2020, 130, 109654.
34. Humblot, V.; Yala, J.-F.; Thebault, P.; Boukerma, K.; Héquet, A.; Berjeaud, J.-M.; Pradier, C.-M., The antibacterial activity of Magainin I immobilized onto mixed thiols Self-Assembled Monolayers. Biomaterials 2009, 30, 3503-3512.
35. Scofield, J. H., Hartree-Slater subshell photoionization cross-sections at 1254 and 1487 eV. Journal of Electron Spectroscopy and Related Phenomena 1976, 8, 129-137.
36. Sauerbrey, G., Verwendung von schwingquarzen zur wagung dunner schichten und zur mikrowagung. Zeitschrift Fur Physik 1959, 155, 206-222.
37. Bizet, K.; Gabrielli, C.; Perrot, H., Immunodetection by quartz crystal microbalance - A new approach for direct detection of rabbit IgG and peroxidase. Applied Biochemistry and Biotechnology 2000, 89, 139-149.

38. Riddles, P. W.; Blakeley, R. L.; Zerner, B., Ellman's reagent: 5,5′-dithiobis(2-nitrobenzoic acid)—a reexamination. Analytical Biochemistry 1979, 94, 75-81.
39. Debiemme-Chouvy, C.; Haskouri, S.; Folcher, G.; Cachet, H., An Original Route to Immobilize an Organic Biocide onto a Transparent Tin Dioxide Electrode. Langmuir 2007, 23, 3873-3879.
40. Ding, Y.; Weng, L.-T.; Yang, M.; Yang, Z.; Lu, X.; Huang, N.; Leng, Y., Insights into the Aggregation/Deposition and Structure of a Polydopamine Film. Langmuir 2014, 30, 12258-12269.
41. Zangmeister, R. A.; Morris, T. A.; Tarlov, M. J., Characterization of Polydopamine Thin Films Deposited at Short Times by Autoxidation of Dopamine. Langmuir 2013, 29, 8619-8628.
42. Chen, T.-P.; Liu, T.; Su, T.-L.; Liang, J., Self-Polymerization of Dopamine in Acidic Environments without Oxygen. Langmuir 2017, 33, 5863-5871.
43. Zheng, W.; Fan, H.; Wang, L.; Jin, Z., Oxidative Self-Polymerization of Dopamine in an Acidic Environment. Langmuir 2015, 31, 11671-11677.
44. Jiang, J.; Zhu, L.; Zhu, L.; Zhu, B.; Xu, Y., Surface characteristics of a self-polymerized dopamine coating deposited on hydrophobic polymer films. Langmuir 2011, 27, 14180-7.
45. Schneider, A.; Hemmerle, J.; Allais, M.; Didierjean, J.; Michel, M.; d'Ischia, M.; Ball, V., Boric Acid as an Efficient Agent for the Control of Polydopamine Self-Assembly and Surface Properties. Acs Applied Materials & Interfaces 2018, 10, 7574-7580.
46. Alfieri, M. L.; Panzella, L.; Oscurato, S. L.; Salvatore, M.; Avolio, R.; Errico, M. E.; Maddalena, P.; Napolitano, A.; D'Ischia, M., The Chemistry of Polydopamine Film Formation: The Amine-Quinone Interplay. 2018, 3, 26.
47. Tanuma, S.; Powell, C. J.; Penn, D. R., Calculation of electron inelastic mean free paths (IMFPs) VII. Reliability of the TPP-2M IMFP predictive equation. 2003, 35, 268-275.
48. Xu, L.; Zuo, Y. Y., Reversible Phase Transitions in the Phospholipid Monolayer. Langmuir 2018, 34, 8694-8700.
49. Yang, W.; Liu, C.; Chen, Y., Stability of Polydopamine Coatings on Gold Substrates Inspected by Surface Plasmon Resonance Imaging. Langmuir 2018, 34, 3565-3571.
50. Del Frari, D.; Bour, J.; Ball, V.; Toniazzo, V.; Ruch, D., Degradation of polydopamine coatings by sodium hypochlorite: A process depending on the substrate and the film synthesis method. Polymer Degradation and Stability 2012, 97, 1844-1849.

51. Pattison, D. I.; Davies, M. J., Absolute Rate Constants for the Reaction of Hypochlorous Acid with Protein Side Chains and Peptide Bonds. Chemical Research in Toxicology 2001, 14, 1453-1464.
52. Peskin, A. V.; Winterbourn, C. C., Kinetics of the reactions of hypochlorous acid and amino acid chloramines with thiols, methionine, and ascorbate. Free Radical Biology and Medicine 2001, 30, 572-579.
53. Su, L.; Yu, Y.; Zhao, Y.; Liang, F.; Zhang, X., Strong Antibacterial Polydopamine Coatings Prepared by a Shaking-assisted Method. Sci Rep 2016, 6, 24420.
54. Iqbal, Z.; Lai, E. P. C.; Avis, T. J., Antimicrobial effect of polydopamine coating on Escherichia coli. Journal of Materials Chemistry 2012, 22, 21608.

Supporting Information

New Antibacterial N-halamine Coating Based on Polydopamine.

Nadia NAZI[1,2], Vincent HUMBLOT*[,1,3], Catherine DEBIEMME-CHOUVY*[,2]

[1] Sorbonne Université, Laboratoire de Réactivité de Surface – UMR 7197, CNRS, 4 place Jussieu, 75005 Paris – France

[2] Sorbonne Université, Laboratoire Interfaces et Systèmes Electrochimiques – UMR CNRS 8235, 4 place Jussieu, 75005 Paris – France

[3] FEMTO-ST Institute, UMR CNRS 6174, Université Bourgogne Franche-Comté, 15B avenue des Montboucons, 25030 Besançon Cedex, France

* Corresponding Authors :

Vincent Humblot, email : vincent.humblot@femto-st.fr, Catherine Debiemme-Chouvy, email catherine.debiemme-chouvy@sorbonne-universite.fr

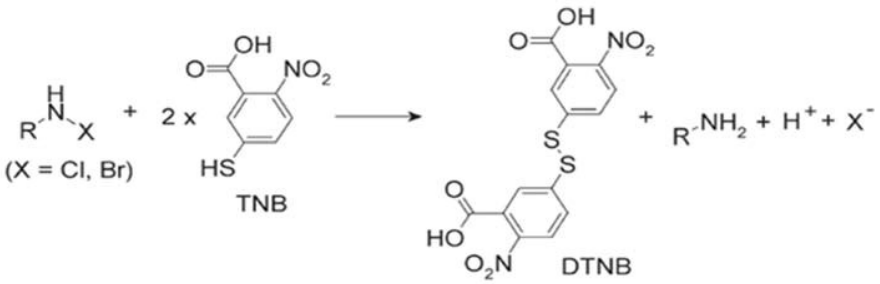

Scheme S1. Reaction between an haloamine compound and TNB.

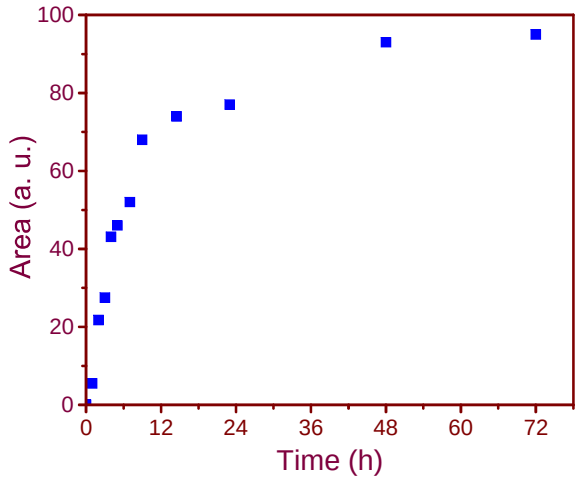

Figure S1. PDA film growth. PM-RAIRS peak area vs. immersion time in a 0.5 mg/mL dopamine solution, data from Fig. 2a.

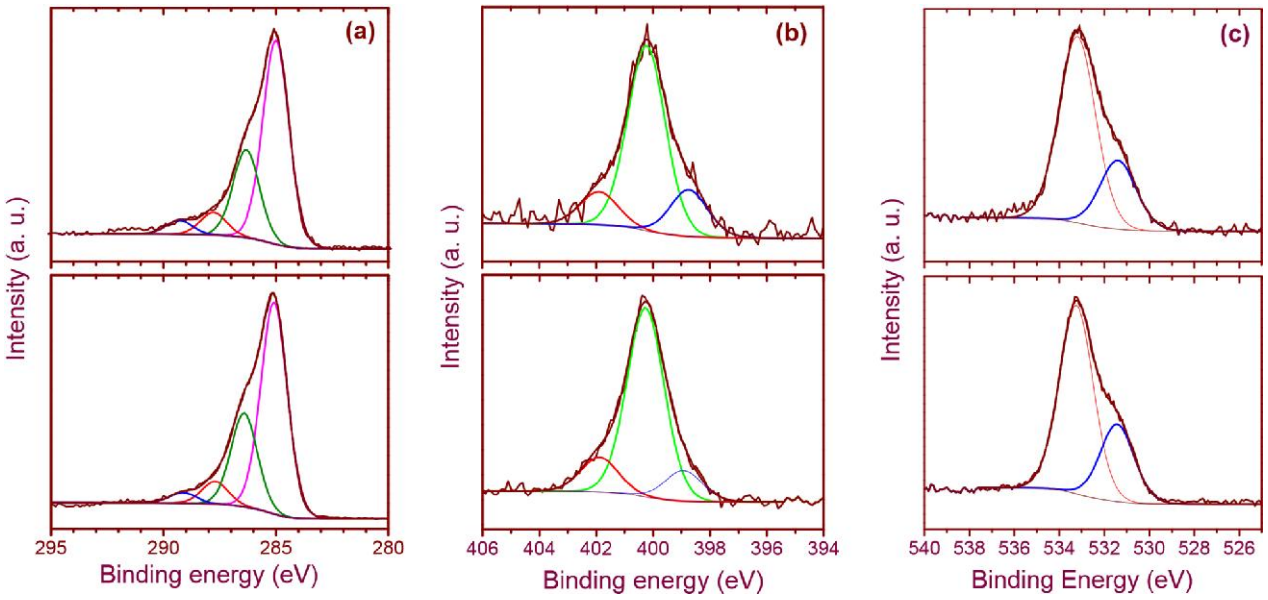

Figure S2. XPS characterizations of modified gold surfaces with PDA films (3 h and 24 h immersion in dopamine solution): (a) C1s, (b) N1s, (c) O1s high-resolution regions. Top: spectra from PDA-3h sample. Bottom: spectra from PDA-24h sample.

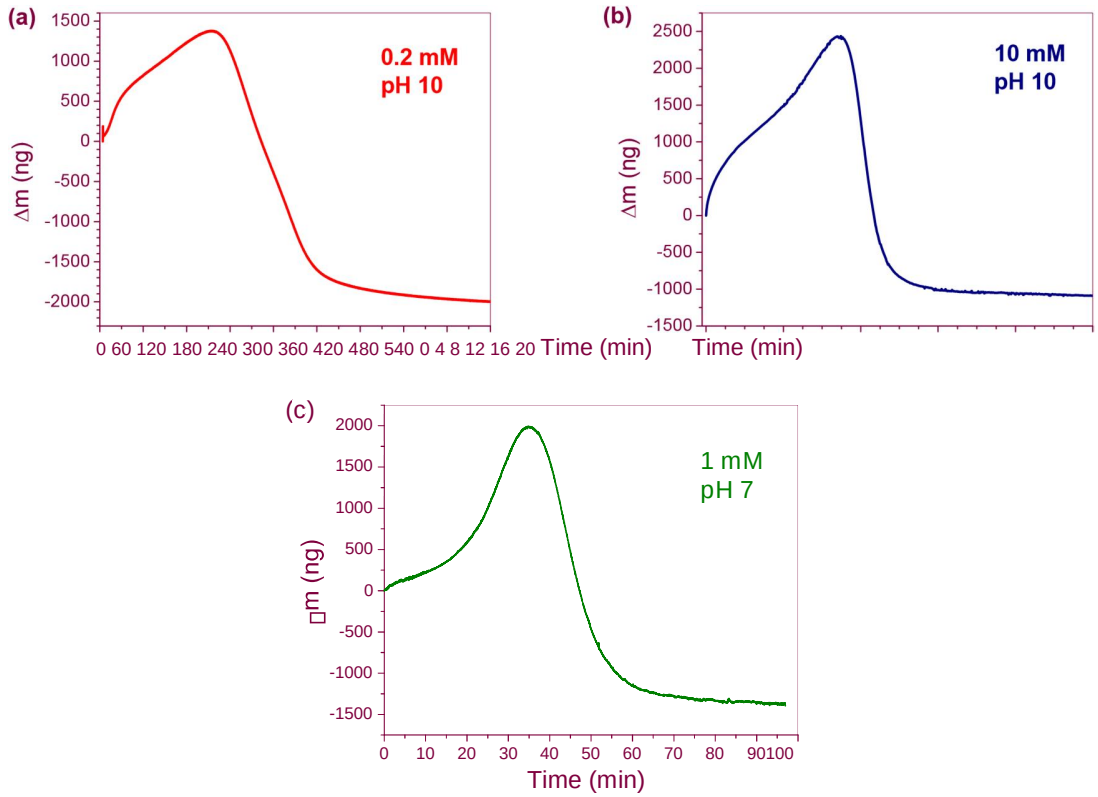

Figure S3. QCM investigation chlorination of PDA-24h film in (a) 0.2 mM, (b) 10 mM NaOCl solution pH 10. (c) 1 mM NaOCl solution pH 7. Quartz area = 0.2 cm^2.

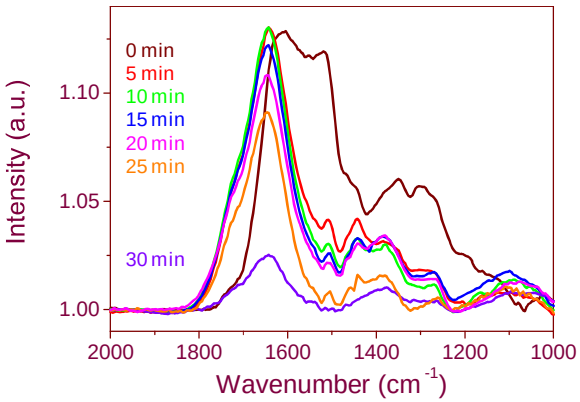

Figure S4. PM-RAIRS spectra of gold surface coated with PDA-3h film as a function of exposure time to a 1 mM NaOCl solution.

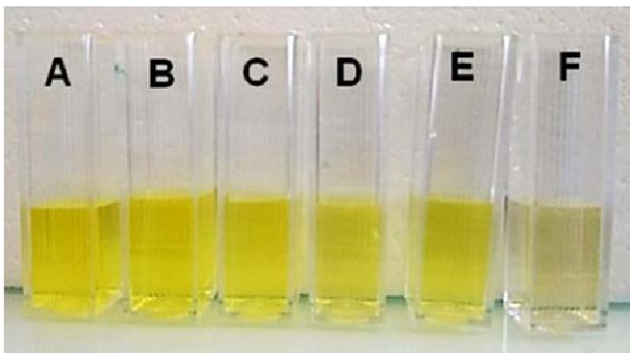

Figure S5. Evidence of chloramine functions: by TNB with Optical image of cuvettes (1 cm) containing the TNB solution after 24h of immersion. (A) unmodified TNB solution. Immersion of (B) Au substrate; (C) PDA-3h film. (D) PDA-3h-Cl film. (E) PDA-24h film and (F) PDA24h-Cl film.

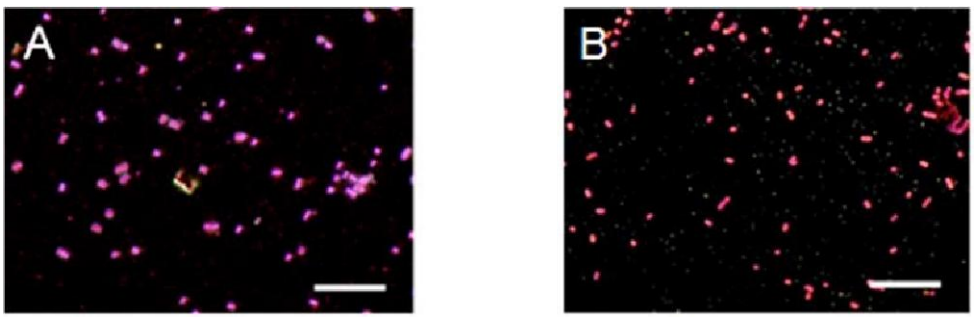

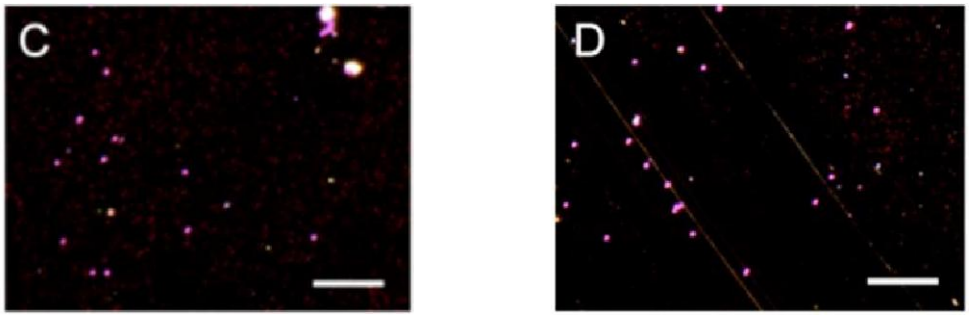

Figure S6. Optical microscopy images in dark field after 17 h at room temperature in contact with E. coli @ 10^7 CFU/mL followed by coloration with crystal violet (A) PDA-3h, (C) PDA3h-Cl, (B) PDA-24 and (D) PDA-24h-Cl. Scale bare: 10 m.

Table S1. Mean CFU/mL of Escherichia coli after killing test on PDA-3h, PDA-24h, chlorinated PDA-3h and chlorinated PDA-24h coatings.

Sample	Inoculum	PDA-3h	PDA-3h-Cl	PDA-24h	PDA-24h-Cl
CFU/mL	$2.50\ 10^7$	$4.66\ 10^5$	$3.84\ 10^5$	$3.58\ 10^5$	$2.36\ 10^5$
% killing /TMX	--	98%	98%	99%	99%
% killing /PDA	--	--	18%	--	34%